Developmental effects of nonuniform acetylcholine receptor expression on motor neuron and synapse morphology in larval zebrafish

By

Nathan R. Nelson

A MASTER'S THESIS

Presented to the Neuroscience Graduate Program

at the Oregon Health and Science University

School of Medicine

In partial fulfillment of

the requirements for the degree of:

Master of Science in Neuroscience

August 17, 2017

School of Medicine

Oregon Health and Science University

We, the thesis committee, hereby certify that the Master's thesis of

Nathan R. Nelson

has been approved

Paul Brehm, Ph.D., Senior Scientist, Thesis Advisor
Vollum Institute for Advanced Biomedical Research

Gail Mandel, Ph.D., Senior Scientist
Vollum Institute for Advanced Biomedical Research

Kevin Wright, Ph.D., Assistant Scientist
Vollum Institute for Advanced Biomedical Research

Haining Zhong, Ph.D., Scientist, Thesis Chairman
Vollum Institute for Advanced Biomedical Research

Table of Contents

Acknowledgements: I will be forever grateful for the all the mentorship I have received from all of my scientific mentors throughout my graduate training starting with my thesis mentor, Paul Brehm Ph.D. PB has always held high expectations in his lab for working hard and producing quality experimental results. PB led by example by being available in lab every day of the week, continually watching over my shoulder with a critical eye to keep me on track with my scientific training. His support of my decision to pursue a Master's degree and an alternative career path reflects his ultimate desire to help his trainees accomplish their goals in order to have a fulfilling career. Hua Wen, Ph.D., has taught me nearly everything I have learned technically in lab, including, but not limited to, zebrafish paired motor-neuron target muscle patch clamp electrophysiology experiments, molecular cloning strategies, genotyping fish lines, designing custom oligonucleotide primer sequences, vital labeling strategies, and confocal imaging. Like PB, Hua has held me to a high standard and pushed me to challenge my scientific and intellectual limits, but she has also been my stronghold in the lab, with the ability to bring a smile to my face in the most stressful of times. I am thankful for Gail Mandel, Ph.D., taking me on as a laboratory technician when I first moved to Oregon and providing me with the freedom to pursue an independent zebrafish electrophysiology project in the Brehm lab, as long as I took care of all my other responsibilities. Gail has also been a wonderful and supportive mentor whenever I had molecular biology questions and am thankful for her contributions to my training as a member of my dissertation advisory committee. I also want to thank Haining Zhong, Ph.D., for his mentorship as the chair of my dissertation advisory committee and for the great experience rotating in his lab in my first year of graduate training. To Kevin Wright, Ph.D., the final member of my

dissertation advisory committee, I am thankful for his mentorship, attention, and interest in my thesis project.

Prior to the commencement of graduate school, Mary Behan, Ph.D., gave me my first job working as a laboratory technician in respiratory neuroscience at the University of Wisconsin – Madison. Mary was an ideal mentor both professionally and personally. It is not possible to portray in words the positive impact Mary's mentorship has had, and continues to have, on my life. I give all credit to my best friend, Keith Hengen, Ph.D., for introducing me to the unique and exciting lifestyle academic neuroscience research can offer; without Keith, I doubt I would have ever discovered academic research, let alone the Behan lab. I have always looked up to Keith as a role model scientist. Keith is quite possibly the only person I have ever met that lives each day of his life at full throttle, passionately giving his all to every component of his multifaceted life; los dos a la muerte! The tremendous amount of support I have received from PB, Gail, Hua, Haining, Kevin, Mary, and Keith has helped me tap into my potential for both professional and personal growth and to realize my capacity to break through my own glass ceilings.

To my parents, Lynn Haucke and Rickey Nelson, I am thankful for their being such wonderful, hardworking, and loving parents and people. Lynn and Rick have independently been, and continue to be, exemplary models of integrity and tenacity, especially during life's most challenging moments. From them, I have learned to always remain positive, honest and to treat others with unconditional respect. My sister Danielle Nelson has taught me to think outside the box, to not fear exploration of life's curiosities, and that anything is possible if you simply commit to your pursuits and remain adaptable to changes throughout the journey. My other family members, Don and Ann Leake as

well as Dave, Dani, Rory and Jameson Dexter, have also been extremely supportive and loving throughout my graduate training. I am a very lucky man to have married into such a fun, easy-going, and wonderful family.

I also want to acknowledge my lab mate and great friend, Benjamin Rakela, Ph.D., who has been a joy to have in the lab. I was fortunate to play a part in teaching Benjamin how to do paired patch clamp recordings when he first came to the Brehm lab as a rotation student. It has been a pleasure and inspiration to work alongside Benjamin over the past five years, watch his progression throughout our graduate training, and see him mature into a skilled and critical scientist. To the rest of my friends outside of lab, I am thankful for their acceptance of my prioritization of my scientific responsibilities and interests above playtime on the nights/weekends and for their loyalty despite the years of missed adventures. Their cumulative friendship and support of my personal and professional endeavors has helped me successfully complete my Master's degree.

Finally, to the love of my life, Claire Leake, a million thanks for all of her patience, love, encouragement, and support throughout my individual and scientific explorations over the past decade as a partner, lab technician, graduate trainee, and husband. I am forever indebted for her choosing to remain by my side and encourage me to sail on as the "seas of science" we have voyaged together would become unexpectedly heavy and relentless. Claire has always helped me chart the best course and navigate back into calmer water. I am fortunate to have the rest of my life to express to Claire all my gratitude and appreciation for her partnership.

ABSTRACT: It is well established that altered postsynaptic receptor activity leads to changes in presynaptic transmission and presynaptic connectivity throughout the nervous system (Turrigiano 2012; Davis and Muller 2015). Receptor-activity-dependent modulation of presynaptic transmission, termed "synaptic plasticity", was first highlighted from studies at neuromuscular synapses and later recapitulated at central synapses (Robbins and Fishbach 1971, Turrigiano 2004, Slater 2015). The receptor-activity-dependent process responsible for reducing the number of presynaptic inputs from multiple neurons onto a target cell throughout synapse development, a form of synaptic competition, was also first demonstrated at the neuromuscular junction (NMJ) (Wyatt and Balice-Gordon 2003) and later observed at central synapses (Kano and Hashimoto 2009). This study, however, probes for evidence of receptor-activity-dependent intra-neuronal competition between axon terminals from the same motor neuron. In this study, I exploit the advantages provided by zebrafish including viable acetylcholine receptor (AChR) null juvenile fish and transparent bodies allowing for direct imaging of spinal motor neurons and neuromuscular synapses. By injecting AChR-δ subunit plasmid cDNA into single cell AChR-null fish embryos, I was able to stochastically rescue AChR expression in a subset of muscle cells (referred to as "partial rescue") to create a unique environment whereby the axon terminals of a single motor neuron will be subjected to nonuniform AChR expression and amounts of AChR activity during development. Using partially rescued AChR-null zebrafish, I tested my hypothesis that primary motor axon terminal morphology and synapse number are dependent on the uniformity of AChR expression and AChR activity. Changes in axon terminal morphology and synapse number were measured from three-dimensional reconstructions

of confocal images. I used this data to determine if there was evidence of AChR-activity-dependent, intra-neuronal competition. AChR-activity-dependent intra-neuronal competition at the developing zebrafish NMJ would provide evidence of a new, intracellular component of receptor-activity-dependent synaptic competition. The findings from this study, however, demonstrate that axon terminal morphology and synapse number are not dependent on either AChR receptor expression or activity. Despite these morphological results, the tools and techniques developed throughout this study provide the possibility to test whether nonuniform AChR receptor expression or activity impact synaptic transmission using patch clamp electrophysiology.

Introduction: It is well established that altered postsynaptic receptor activity leads to changes in presynaptic transmission and presynaptic connectivity throughout the nervous system (Turrigiano 2012; Davis and Muller 2015). Receptor-activity-dependent modulation of presynaptic transmission, termed "synaptic plasticity", was first highlighted from studies at neuromuscular synapses and later recapitulated at central synapses (Robbins and Fishbach 1971, Turrigiano 2004, Slater 2015). The receptor-activity-dependent process responsible for reducing the number of presynaptic inputs from multiple neurons onto a target cell throughout synapse development, a form of synaptic competition, was also first demonstrated at the neuromuscular junction (NMJ) (Wyatt and Balice-Gordon 2003) and later observed at central synapses (Kano and Hashimoto 2009). My study, however, probed for evidence of receptor-activity-dependent intra-neuronal competition between axon terminals from the same motor neuron.

In this study, I exploit the advantages provided by zebrafish, including viable acetylcholine receptor (AChR) null juvenile fish and transparent bodies that allow for direct imaging of spinal motor neurons and neuromuscular synapses. By injecting AChR-δ subunit plasmid cDNA into single cell AChR-null fish embryos, I was able to stochastically rescue AChR expression in a subset of muscle cells (referred to as "partial rescue") to create a unique environment whereby the axon terminals of a single motor neuron can be subjected to nonuniform AChR expression and amounts of AChR activity during development. Using partially rescued AChR-null zebrafish, I tested my hypothesis that primary motor axon terminal morphology and synapse number are dependent on the uniformity of AChR expression and AChR activity. Changes in axon terminal

morphology and synapse number were measured from three-dimensional reconstructions of confocal images. I used this data to determine if there was evidence of AChR-activity-dependent, intra-neuronal competition. AChR-activity-dependent intra-neuronal competition at the developing zebrafish NMJ would provide evidence of a new, intracellular component of receptor-activity-dependent synaptic competition.

AChR inactivity is consequent to denervation supersensitivity: The involvement of AChR activity in maintaining localized muscle sensitivity to acetylcholine (ACh) at the endplate was discovered through studies of denervated muscle. AChR inactivity at denervated synapses of adult mammalian muscle consistently results in increased muscle sensitivity to exogenous ACh. Brown (1937) offered the earliest evidence of increased cholinergic sensitivity through electromyographic recordings of muscle activity from denervated cat muscle following arterial injection of ACh. Brown reported that denervated muscle could be excited by an ACh concentration 1,000 times less than that required to excite intact muscle. Subsequent testing of membrane sensitivity to ACh at higher resolution showed that denervated muscle induced ACh sensitivity throughout the extrasynaptic membrane. Axelsson and Thesleff (1959) iontophoretically applied ACh to distinct locations along the muscle membrane while acquiring intracellular recordings from isolated cat muscle. They observed that denervated muscle became sensitive to ACh outside the endplate region based on membrane depolarizations in response to puffs of ACh all along the muscle. This observation was in stark contrast to controls where iontophoretic ACh could depolarize

the membrane only when directly applied to the endplate. From these findings Axelsson and Thesleff proposed that synaptic activity limits ACh sensitivity to the endplate.

Muscle membrane hypersensitivity to ACh was then directly linked to AChR activity through functional blockade of cholinergic transmission. In separate experiments, Berg and Hall (1975) used an irreversible AChR antagonist alpha-bungarotoxin (αBTX) and a reversible AChR antagonist, d-tubocurarine (curare), to chronically block AChR activity in rat muscle. By measuring the amount of radiolabeled AChRs from dissected endplate-free muscle, they found that cholinergic blockade in each condition was as effective at inducing increases in extrasynaptic AChR expression as that induced by denervation. Using the same method to measure extrasynaptic AChRs, Pestronk et al. (1976) prevented evoked ACh release by blocking presynaptic action potentials with tetrodotoxin (TTX). Decreasing cholinergic activity with TTX also increased the amount of extrasynaptic AChRs compared to controls. However, Pestronk et al. noted that TTX treatment was less effective at inducing increases in extrasynaptic AChR expression compared with their denervation experiments. The lesser effects observed with TTX were likely a consequence of small amounts endplate AChR activity in response to spontaneously released ACh. These results suggest that the suppression of extrasynaptic AChR expression depends on AChR activity. Thus, the discovery that maintenance of ACh sensitivity to the mature endplate is dependent on AChR activity opened the door to thinking that AChR activity could also play a major role in synapse development.

AChR activity mediates synaptic elimination: The detection of axon elimination through electrophysiological recordings of developing muscle led to evidence

that AChR activity also plays an important role in reducing supernumerary presynaptic endplate innervation (Redfern 1970). At most embryonic NMJs, axon terminals from different motor neurons converge onto and polyinnervate the endplate region. Supernumerary innervation of immature endplates was determined through intracellular recordings of evoked end plate potentials (EPPs) in response to incremental electrical stimulation of motor nerves. As the stimulus strength increased, neural inputs were sequentially recruited, resulting in graded levels of endplate depolarization.

The number of synaptic inputs to an immature endplate was reflected by discrete increases in the EPP amplitude recorded from the same muscle. EPPs of increasing amplitude in response to graded stimulation are characteristic of polyinnervated endplates and are referred to as compound EPPs (Redfern 1970). In contrast, mature endplates are monoinnervated therefore all stimulus intensities would yield EPPs with similar amplitudes. Redfern (1970) was the first to observe the gradual loss of compound EPPs from rat muscle, isolated from birth to one month of age. Subsequently, Brown et al. (1976) observed a similar step-wise disappearance of compound EPPs from maturing rat soleus muscle. They suggested that the gradual elimination of axonal inputs at the developing NMJ was determined through competitive interactions between the axon terminals from different motor neurons. Axon elimination has since, been extensively studied and is now widely accepted to be the outcome of a developmental process known as synaptic competition (Colman and Lichtman 1993).

AChR activity mediates inter-neuronal synaptic competition: Based on previous studies that demonstrated the dependence of AChR activity in preventing the

expression of extrasynaptic AChRs (Berg and Hall 1975, Pestronk et al. 1976), tests for a mechanism underlying synaptic competition began by altering AChR activity. Thompson et al. (1979) reduced AChR activity at the rat NMJ by blocking evoked ACh release with TTX. Following a prolonged decrease in synaptic activity, they found that the onset of axon elimination was delayed based on the persistent appearance of compound EPPs. This was the first functional evidence in support of AChR activity serving an important role in the mechanism underlying synaptic competition. The findings from Thompson et al. suggest that decreased AChR activity reduces the intensity of synaptic competition between axon terminals. If the amount of AChR activity modulates the amount of synaptic competition, then increasing the amount of AChR activity at the developing NMJ would be expected to enhance the competitive interactions between axon terminals and thus accelerate axon elimination.

This hypothesis was supported by Thompson (1983), based on observations that compound EPPs disappear more rapidly following increased evoked synaptic transmission during a period when the muscles of rat pups are normally polyinnervated. In this study, stimulating electrodes were implanted to drive motor nerve activity with prolonged stimulation and muscles were later isolated for intracellular recording. Based on the recording of fewer compound EPPs, Thompson found that increased motor nerve activity reduced the amount of polyneuronal innervation by about 50% compared to age-matched controls.

Additional support for the dependence of AChR activity in modulating synaptic competition is based on histological evidence of changes in both pre- and post-synaptic morphology following prolonged partial blockade of endplate AChR activity. Balice-

Gordon and Lichtman (1994) used rhodamine-conjugated αBTX to label AChRs and visualize the endplate region of polyinnervated mouse muscle. With the muscle under constant perfusion, unlabeled αBTX was puffer-applied to a portion of the endplate to block a subset of the AChRs in order to avoid complete blockade of all endplate AChRs. As endplate AChRs are known to turn over with a half-life of 30 hours (Burden 1977), it was important to repeatedly block the same portion of the endplate over a series of days. A final labeling of all unblocked endplate AChRs with fluorescent αBTX revealed that functional AChRs were only expressed within unblocked endplate regions. Presynaptic motor inputs to the same endplates were visualized by using a vital mitochondrial dye and were found to be exclusively located opposite the endplate regions containing fluorescently labeled AChRs. This evidence suggests that nonuniform amounts of AChR activity within the endplate region are capable of mediating axon elimination. Collectively, the findings from studies of synaptic competition show that AChR activity at the endplate is important for reducing presynaptic connectivity at the developing NMJ.

Intra-neuronal synaptic competition and AChR activity: While the AChR-activity-dependent process of synaptic competition just described pertains to the competitive interactions between axon terminals from different neurons (inter-neuronal) throughout synapse development, I set out to determine if there are AChR-activity-dependent, competitive interactions between axon terminals within the same neuron; this will be referred to as intra-neuronal competition. AChR-activity-dependent intra-neuronal competition at the developing zebrafish NMJ would provide evidence of a novel component of receptor-activity-dependent synaptic competition. In this study I used

AChR-null zebrafish as they represent the only viable AChR-null model system in vertebrates (Li et al. 2003; Westerfield et al. 1990; Witzemann et al. 2013) and rescue of AChRs in AChR-null fish has been previously demonstrated (Ono et al. 2004; Epley et al. 2008). Zebrafish also have transparent bodies allowing for direct imaging of spinal motor neurons and neuromuscular synapses. Furthermore, zebrafish neuromuscular connectivity is well defined whereby the caudal primary (CaP) motor neuron is the only primary motor neuron within each myotomal segment along the length of the fish body that projects its extensive arbor of axon branch terminals to a corresponding region of ventral skeletal muscle, forming en passant synapses with AChR clusters throughout the target ventral musculature (Westerfield et al. 1986; Beattie 2000).

In this study I tested for changes in CaP axon terminal morphology and synapse number in response to nonuniform AChR expression in partially rescued AChR-null zebrafish. Partial rescue of a subset of ventral muscle cells would result in nonuniform expression of AChRs throughout the target muscle field. As a consequence of nonuniform AChR expression, CaP axon terminals would be subjected to nonuniform levels of AChR activity throughout the target muscle field. Morphological changes in CaP axon terminal morphology and synapse number in response to nonuniform AChR expression would provide evidence of intra-neuronal competition and improve our understanding of the mechanisms underlying synaptic competition during neuromuscular development.

I used homozygous mutant *sofa potato* zebrafish that are AChR-null (Ono et al. 2001) due to a point mutation in the gene encoding the AChR-δ subunit (Ono et al. 2004). AChRs are pentameric proteins typically comprising four different subunits

(embryonic isoform: $\alpha_2\beta\delta\gamma$, adult isoform: $\alpha_2\beta\delta\varepsilon$; Mishina et al. 1986; Mongeon et al. 2011) and it has been shown that the mutation in the AChR-δ subunit gene in *sofa potato* mutants prevents the expression of functional AChRs in muscle cells. While most other vertebrate AChR-null models are embryonic lethal (Li et al. 2003; Witzemann et al. 2013), paralytic AChR-null zebrafish are viable and survive for 5 – 7 days, well beyond the time required for development of mature neuromuscular synapses in wild-type fish (Westerfield et al. 1990; Ono et al. 2001). Rescue of AChR expression in *sofa potato* mutants has been previously demonstrated by injecting wild-type AChR-δ subunit plasmid complementary deoxyribonucleic acid (cDNA) into *sofa potato* mutant embryos at the single-cell stage (Ono et al. 2004; Epley et al. 2008).

The ability to manipulate AChR expression in an AChR-null background makes zebrafish an ideal model system to address the question of receptor-activity-dependent changes in axon terminal and synapse morphology. For my experiments, I have used this cDNA injection method to mosaically rescue AChR expression in muscle cells in *sofa potato* mutants. Rescue of AChR expression occurs exclusively in muscle cells due to the AChR-δ subunit gene being driven by the zebrafish muscle-specific promoter, α-actin (Higashijima et al. 1997). Nuclear uptake of the AChR-δ subunit plasmid into the dividing cells of the developing embryo is a random process; therefore the transcription of AChR-δ subunit mRNA, translation of AChR-δ subunit protein, and assembly of AChR-δ subunit protein into functional pentameric AChRs were stochastically distributed throughout the muscle cells of partially rescued *sofa potato* mutants (Fig. 1B).

The rescue plasmid also contains the cDNA encoding cytoplasmic enhanced green fluorescent protein (EGFP) that co-expresses with the AChR-δ subunit within

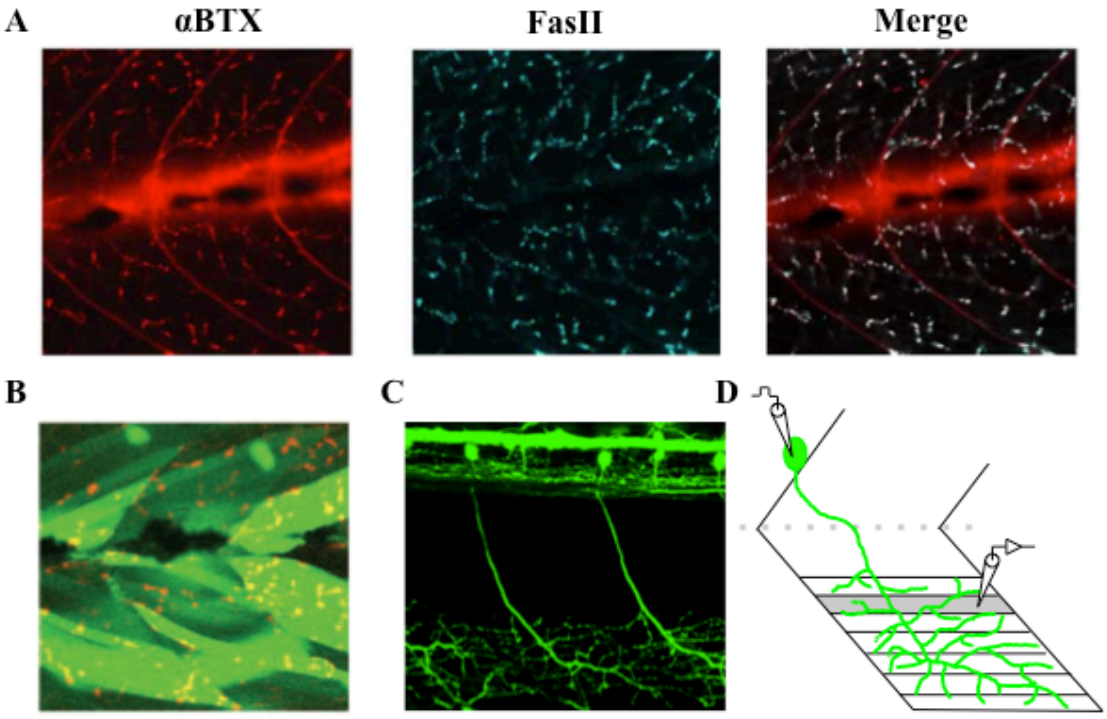

Figure 1. (**A**) Example images of directly labeled AChRs with fluorescent αBTX (left), AChE with fluorescent FasII (middle), and the colocalization of both postsynaptic indicators in a merged image (right) (taken from Wen and Brehm 2005). (**B**) Example image of mosaic pattern of muscle GFP fluorescence (green) and associated rescued AChRs labeled with fluorescent αBTX (red) in a *sofa potato* mutant fish (taken from Ono et al. 2004). (**C**) Specificity of cytoplasmic GFP expression in the CaP spinal motor neurons of wild-type;SAIG fish (Wen et al. 2015). (**D**) Schematic of a paired recording between the CaP motor neuron (green) and a rescued target ventral muscle cell (grey) on the left side of a partially rescued *sofa potato* mutant fish. Dotted grey line marks the dorsal/ventral myotomal divide along the midline of the fish body.

rescued muscle cells. Based on Ono et al. (2004), using this same AChR-δ subunit plasmid in *sofa potato* mutants, the cells expressing detectable EGFP fluorescence appeared to consistently express AChRs (Fig. 1B). Paired recordings were used to determine if the level of muscle EGFP fluorescence correlated with the level of functional rescue. For this purpose, single-cell *sofa potato* embryos were injected with different concentrations of the AChR-δ subunit plasmid (10 – 50 pg) to vary the degree of mosaic muscle rescue and electrophysiological recordings were performed at 3 days post fertilization (dpf). At this time point, CaP axon terminal branches project throughout the ventral, target muscle field (Fig. 1C; Wen et al. 2015) and synapses predominantly contain adult isoform AChRs (Walogorsky et al. 2012). Synaptic currents from rescued muscle were recorded and the amplitudes of evoked endplate currents (EPCs) were compared the to the brightness of muscle EGFP fluorescence.

To test for changes in CaP axon morphology and synapse number in response to nonuniform AChR expression, I first established the morphological characteristics of CaP axons under control conditions using transgenic wild-type;SAIG fish, which have CaP motor axons that exclusively express cytoplasmic GFP (Wen et al. 2015). To identify individual synaptic puncta I directly injected either Alexa Fluor 568, or 647, conjugated αBTX (αBTX-568/647) or Alexa Fluor 647 conjugated fasciculin II (FasII-647), or both αBTX-568 and FasII-647, into the circulatory system, to label AChRs and acetylcholinesterase (AChE), respectively (Fig. 1A; Wen and Brehm 2005; Wen et al. 2015). AChE serves as a permanent marker of synapses (McMahan et al. 1978), which provides the advantage of marking the location of putative synapses in the event presynaptic axon terminals retract from the muscle in response to nonuniform AChR

expression. Thus, labeling AChE with FasII-647 provided the ability to visualize postsynaptic sites on both rescued and non-rescued muscle cells.

Following injection of αBTX-568/647 and/or FasII-647, z-stack confocal images of the CaP axon terminal arbor were acquired and images were three-dimensionally reconstructed using Imaris Filament Tracer software (version 8.4.2, Bitplane, Zurich, Switzerland). The total number of axon branches throughout the CaP axon terminal arbor and the number of αBTX puncta on rescued muscle cells were quantified. In wild-type;SAIG fish, I expected to see normal CaP axon terminal branching throughout the target muscle field (Fig. 2A) as well as ubiquitous punctate fluorescence of αBTX (Fig. 1A left; Fig. 2B) and FasII (Fig. 1A middle; Fig. 2C) on all ventral muscle cells. Furthermore, fluorescent puncta from both postsynaptic indicators were expected to colocalize at all postsynaptic sites throughout the target muscle field in wild-type fish (Fig. 1A right; Fig. 2D). I then repeated these experiments using transgenic *sofa potato*;SAIG fish line to establish the morphological characteristics of postsynaptic sites and CaP axon terminal branching in non-rescued *sofa potato* mutant fish. It was previously suggested that motor axon morphology of *sofa potato* mutant fish appears qualitatively normal (Westerfield et al. 1990, Ono et al. 2001, Li et al. 2003). Precedent for this result comes from a different study that found no changes presynaptic morphology when the activity of all endplate AChRs was blocked with αBTX at the mouse NMJ (Balice-Gordon and Lichtman 1994). Therefore, I expected the CaP axonal terminal arbor of non-rescued *sofa potato* mutants to be similar to wild-type fish both qualitatively and quantitatively (Fig. 2E). Postsynaptically, there should be no αBTX puncta on the muscles of AChR-null *sofa potato* mutants, as expected (Fig. 2F).

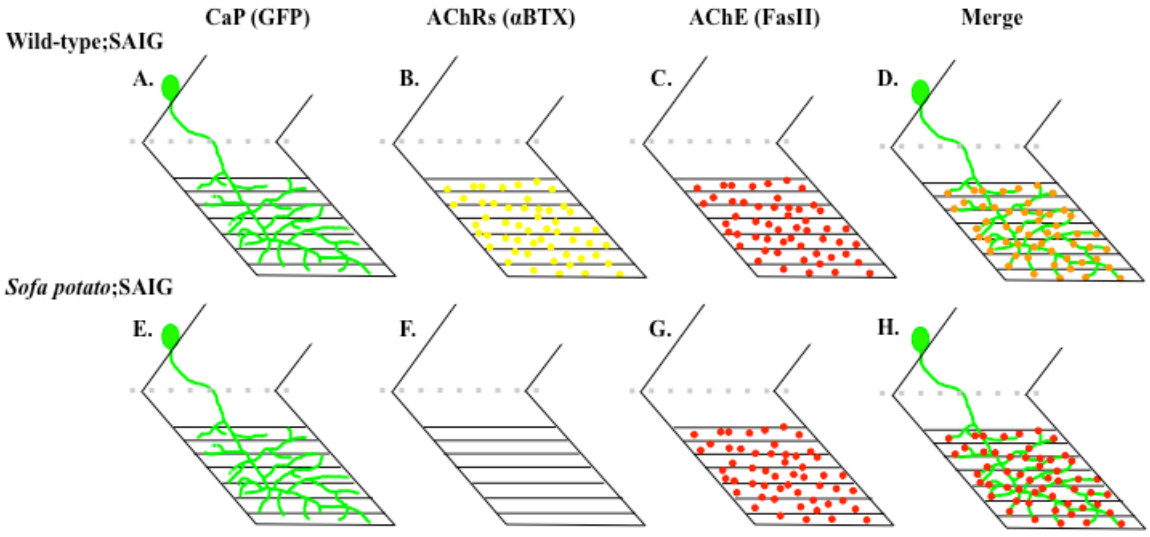

Figure 2: Schematic of expected CaP axon terminal branch morphology (CaP GFP – green) and distribution of AChR (αBTX – yellow) and AChE (FasII – red) expression in wild-type and AChR-null *sofa potato* controls. Dotted grey line marks the dorsal/ventral myotomal divide along the midline of the fish body. (**A-D**) wild-type;SAIG (**E-H**) non-rescued *sofa potato*;SAIG. CaP axon terminal branch morphology should be similar between wild-type and *sofa potato* fish (**A** & **E**). Expression of αBTX labeled AChRs (**B**) and FasII labeled AChE (**C** & **G**) should colocalize along the CaP axon terminal branches in merged images (**D** & **H**).

However, I did predict observing FasII puncta (Fig. 2G) located along the axon terminal branches throughout the CaP axonal terminal arbor (Fig. 2H), as AChE does not require the presence of AChRs for expression and localization (Ibanez-Tallon et al. 2004). To test for morphological changes associated with nonuniform AChR expression, I used partially rescued *sofa potato*;SAIG mutants that had been injected with the AChR-δ subunit plasmid at the embryonic single-cell stage. Quantitative and qualitative analyses of CaP axon terminal morphology and synapse number in partially rescued *sofa potato*;SAIG mutants were compared to wild-type;SAIG and non-rescued *sofa potato*;SAIG mutants.

I verified whether CaP axon terminal morphology and synapse number were altered in response to nonuniform AChR expression in partially rescued *sofa potato*;SAIG mutants by counting number of axon terminal branches throughout the CaP axon terminal arbor to quantify the extent of CaP axon terminal arborization. Then, within each CaP-associated ventral myotome, I quantified the number of αBTX puncta on individual identified muscle cells. Through both qualitative comparisons of pre- and post-synaptic morphology and quantitative comparisons of the number of synapses and the number of CaP axon terminal branches, I determined which of the proposed models corresponded to the actual experimental outcomes. Finally as an optical assay of functional differences in presynaptic transmission, which may be the consequence of nonuniform AChR activity, I tested for differences in presynaptic vesicle recycling by loading axon terminal boutons with FM1-43. The punctate expression of FM1-43 loaded presynaptic boutons was reconstructed similarly to αBTX and FasII puncta to assess if presynaptic vesicle recycling is different between rescued and non-rescued synapses.

Methods:

Fish: Day 3 – 5 (72 – 120 hour post fertilization (hpf)) wild-type or *sofa potato* mutant zebrafish (*Danio rerio*) were used in this study. SAIGFF213A/UAS:GFP double-transgenic wild-type (wild-type;SAIG; Muto et al. 2011) fish, which express cytoplasmic GFP in their CaP motor neurons, were used for confocal imaging experiments. Heterozygous adult *sofa potato* fish were crossed with wild-type;SAIG fish, in house, to create a *sofa potato*;SAIG fish line. Identified *sofa potato*;SAIG heterozygous adults were used to generate mutant embryos for partial rescue experiments.

Obtaining *sofa potato* mutant embryos: Adult (>3 mo.) heterozygous *sofa potato* fish were identified either individually by detection of the mutant allele in genomic DNA extracted from tail fin clips or as breeding pairs as the ~25% of the offspring from a male and female heterozygous *sofa potato* fish have a paralytic phenotype. Identified heterozygous *sofa potato* fish were in-crossed to obtain homozygous mutant embryos for experimentation.

Genotyping adult heterozygous *sofa potato* fish by fin clip: Adult fish were briefly anesthetized in 0.02% tricaine, transferred to a clean glass surface and a small piece of the tail fin was cut off and placed into a 0.2 ml polymerase chain reaction (PCR) tube. Fin clips were submerged in lysis buffer and digested overnight at 55° F to extract genomic DNA. The following morning, the proteinase-k in the lysis buffer was heat-inactivated and samples were prepared for PCR amplification of a 176 base pair (bp)

region of genomic DNA surrounding the location of the point mutation in the *sop tj*^{19d} mutant allele using the forward- 5' - AGC ACT CAC CAA GGA AAT GAG - 3' and reverse-primers 5' - GAC TTG CAG TGT GTT TTG CAG - 3'. This point mutation creates a recognition site in the mutant allele for the BccI restriction endonuclease (5' - CCA TC(N) - 3') that is absent in fish lacking the mutant allele. The PCR product is then subjected to BccI restriction digest and samples were loaded into an agarose gel for electrophoresis. Digested DNA from heterozygous *sofa potato* fin clips yield three fragments (58, 115, and 176 bp) whereas DNA from wild-type like *sofa potato* fish yield only one full-length fragment (176 bp).

α-Actin-AChR-δ-P2A-mCherry plasmid design: In order to identify rescued muscle cells that expressed functional AChRs, Hua Wen Ph.D., Katie Drerup Ph.D. and I created a bicistronic cDNA plasmid where both the AChR-δ subunit and the mCherry transcripts were driven by the zebrafish-muscle specific promoter α-actin, separated by a 22 bp P2A sequence (Kim et al. 2011). Using the Gibson cloning method, the α-actin promoter was assembled into the 5' Entry vector and the P2A-mCherry was assembled into the 3' Entry vector. The AChR-δ subunit was inserted into the pDONR221 Middle Entry vector using Gateway recombination. An LR reaction was subsequently performed to generate the final α-actin-AChR-δ-P2A-mCherry clone.

Primers:

α-actin (XhoI) forward: 5' - CTC GAG GTC GAC GGT AT - 3'

α-actin (SacII) reverse: 5' - CCC GGG GAT GGC CGC TCT AG - 3'

AChR-δ BP forward: 5’ - GGG GAC AAG TTT GTA CAA AAA AGC AGG CTA TGA TGA AAA CTG TTC - 3’

AChR-δ BP reverse: 5’ - GGG GAC CAC TTT GTA CAA GAA AGC TGG GTA CAA ATA GCG CCT GTT T - 3’

Plasmid injections and screening for confocal imaging: To fluorescently label individual muscle cells in wild-type fish, 50 pg of α-actin-mCherry cDNA was pressure injected into the yolk of single-cell wild-type;SAIG embryos. To partially rescue AChR expression in muscle cells, and fluorescently label rescued muscle cells in *sofa potato* fish, 50 pg of α-actin-AChR-δ-P2A-mCherry was pressure-injected into single cell *sofa potato* or *sofa potato*;SAIG embryos. At 1 dpf, transgenic fish were screened for expression of GFP fluorescence in the spinal cord and *sofa potato* embryos were dechorionated to screen for paralytic mutants in response to mechanical stimulation (Ono et al. 2001). At 3 dpf, plasmid injected embryos are ultimately screened for muscle expression of mCherry fluorescence in ~1 – 3 muscle cells per ventral segment. Identified embryos are subsequently imaged at either 3 or 5 dpf.

Fish preparation for electrophysiology: Under a stereo microscope (Leica S8 APO, Leica Microsystems, Buffalo Grove, IL), fish were anesthetized with 0.02% tricaine, decapitated at the midpoint of the yolk sac, and secured to a Sylgard-coated recording chamber using electrolytically sharpened tungsten pins through the notochord. Bathed in 3 ml of bath recording solution (BRS), the skin of the fish was pulled up at the rostral pin using a small hook and carefully removed by pulling the skin towards the tail

with fine forceps. During a brief (4 min) solution exchange for BRS containing 10% formamide (2 M), dorsal muscle cells were gently brushed away using the tip of a nose-hair to expose the dura of the spinal cord. Subsequently, the osmotic shock of 5, 3 ml washes of BRS disrupts excitation-contraction coupling in the intact ventral muscle cells to minimize contraction during electrophysiological recording (del Castillo and de Motta 1978). The preparation was then placed on a fixed stage, upright microscope (Zeiss Axio Examiner D.1, Carl Zeiss, Oberkochen, Germany) whereby Kohler illumination was optimized for a 40x/0.8 W objective (Zeiss 440095) and the image profile was displayed on a dc-video monitor via CCD camera (DAGE-MTI IR-1000, Michigan City, IN) for further dissection. Microelectrodes (TW150F, World precision instruments, Sarasota, FL) were pulled using a vertical pipette puller (Tower of Power) to create suction pipettes; the tip of the pipette was melted and bent into a hook to hold a small weight by which subsequent heat pulses yielded a clean, broken tip of ~20 μm diameter (MF-79 Narishige micro-forge, Tokyo, Japan). Excess muscle debris was vacuumed from the body wall by means of negative pressure created manually via a 5 ml syringe. Superficial, slow muscle cells were also removed from the ventral side to gain access to the deeper layers of fast muscle that are innervated by the CaP motor neuron.

Solutions:

Bath recording solution (BRS; in mM): 134 NaCl, 2.9 KCl, 2.1 $CaCl_2$, 1.2 $MgCl_2$, 10 dextrose, 10 Na-HEPES, pH 7.4 with NaOH, 290 mOsm.

High-K BRS (in mM): 92 NaCl, 45 KCl, 2.1 $CaCl_2$, 1.2 $MgCl_2$, 10 dextrose, 10 Na-HEPES, pH 7.4 with NaOH, 290 mOsm.

Low-Ca^{2+} BRS (in mM): 134 NaCl, 2.9 KCl, 0.5 $CaCl_2$, 2.8 $MgCl_2$, 10 dextrose, 10 Na-HEPES, pH 7.4 with NaOH, 290 mOsm.

Spinal motor neuron/muscle internal solution (in mM): 115 K-gluconate, 15 KCl, 2 $MgCl_2$, 4 Mg-ATP, 5 EGTA, 10 K-HEPES, pH 7.2 with KOH, 290 mOsm.

Patch clamp electrophysiology to test rescue plasmid: Whole cell patch clamp recordings of CaP motor neurons were performed using a HEKA EPC 10/2 amplifier (Heka Electronik, Lambrecht/Pflaz, Germany) as described (Wen and Brehm 2005, 2010). In brief, patch electrodes (1B150F-4, World precision instruments, Sarasota, FL) were pulled on a horizontal pipette puller (P-97 Flaming/Brown Micropipette Puller, Sutter Instruments, Novato, CA) to obtain a long, narrow shank with a tip of ~1 μm (12 – 18 MΩ resistance). If transgenic SAIG fish were not used, Alexa Fluor 488 hydrazide dye (40 μM) was often added to the spinal motor neuron internal solution for morphological reconstruction of the CaP. Under positive pressure (DPM-1B Fluke Pneumatic Transducer, Fluke Biomedical, Everett, WA), the recording electrode was pierced through the spinal cord dura and brought in contact with the soma of the identified CaP motor neuron. A high resistance GΩ-seal with the cell membrane was formed upon removal of positive pressure, and subsequent light, negative pressure was orally applied until whole cell access is gained. The CaP membrane potential was held at

-80 mV in voltage clamp. Preliminary confirmation of CaP motor neuron identity was based on three metrics: (1) an input resistance of ~150 – 200 MΩ in the whole cell configuration, (2) the amount of current injection (2 ms, 50 pA steps) required to evoke an action potential (~300 – 450 pA), and (3) the characteristic shape of the action potential waveform while in the current clamp configuration with a peak amplitude of +60 mV (Fig. 3). Whole cell voltage clamp recordings of ventral fast skeletal muscle utilized patch electrodes pulled to have a short shank with a tip diameter of ~3 μm (3 – 5 MΩ tip resistance). Muscle cells were held at -80 mV to inactivate voltage-gated sodium channels and increase the driving force for recording EPCs. Paired CaP motor neuron target muscle recordings were confirmed by evoking action potentials in the CaP and recording the evoked, synchronous EPCs (Fig. 3).

Vital labeling of AChRs and AChE with fluorescently conjugated αBTX and FasII: Fish were individually oriented in a tissue culture dish filled with slanted agarose to visualize the lateral dorsal aorta that runs between the otolith organ and the yolk sac. A microinjection pipette was loaded with either 0.1 mg/ml fluorophore conjugated αBTX or 0.14 mg/ml FasII and injection volumes were calibrated to 10 nl. The injection needle was pierced through the skin into the lateral dorsal aorta and the fluorescent toxin was pressure-injected into the bloodstream. Perfusion of the injected toxin throughout the circulatory system allowed for vital labeling of AChRs and AChE with αBTX and FasII, respectively. Fish were then monitored for complete paralysis, upon which complete binding of fluorescent toxin and thus labeling of AChRs or AChE was assumed.

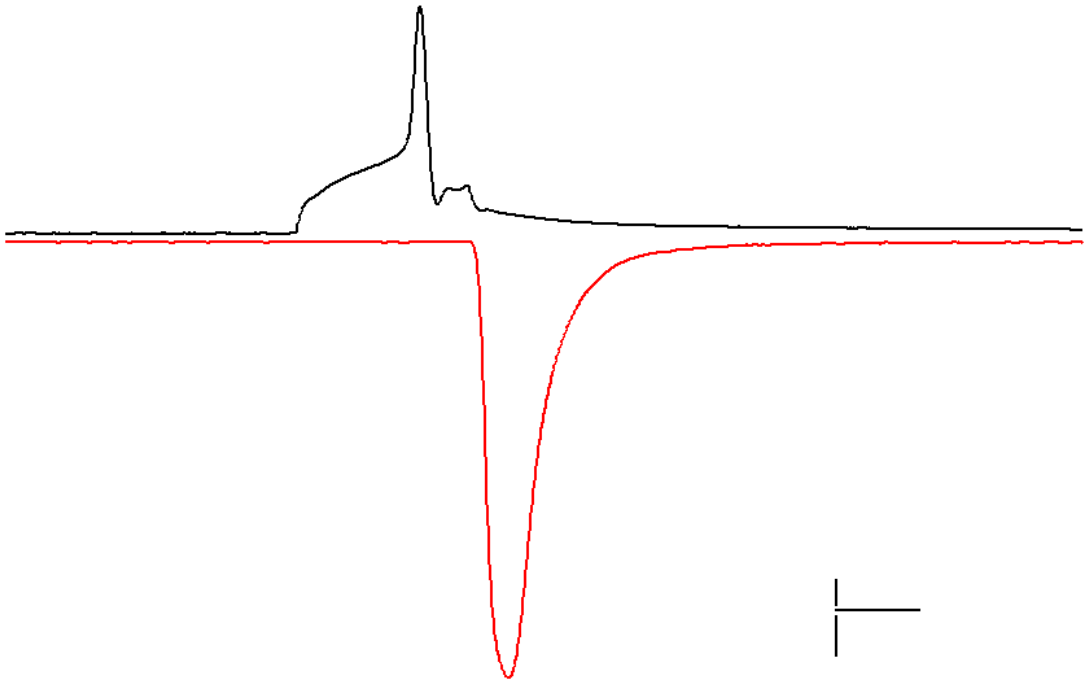

Figure 3. Paired motor neuron-muscle recording showing an action potential from a CaP motor neuron (black) and an evoked EPC from a target fast muscle cell (red). Scale bar: 20 mV (top), 1 ms (middle), and 2 nA (bottom).

Loading motor axon terminal boutons with vital dye FM1-43: Live fish were anesthetized in embryo media containing 0.02% tricaine and transferred to a dish filled with BRS. With the head intact, half of the skin was removed as described above. Fish were transferred to a dish containing 0.1 μM αBTX-647, to label AChRs and minimize contraction of muscles from spontaneous vesicle release, and 10 μM FM1-43, to preload the dye into the interstitial spaces. Fish were then transferred to High-K BRS containing 10 μM FM1-43 to load recycling synaptic vesicles, and subsequently transferred to BRS containing 10 μM FM1-43 and 1 μM TTX. Fish were then subjected to a series of washes with Low-Ca^{2+} BRS containing 1 μM TTX and 1 mM Advasep-7 to minimize destaining of loaded synaptic vesicles and remove residual FM1-43 from the interstitial spaces. After a final series of washes with Low-Ca^{2+} BRS containing 1 μM TTX, fish were mounted for confocal imaging as described below.

Live confocal imaging: Fish were mounted on a glass coverslip in 1.4% low-melt agarose for confocal imaging (Zeiss LSM 710). When the agarose solidified, the dish was filled with embryo media to prevent movement artifacts due to evaporation of the agarose. Using a 63x/1.2 W objective (Zeiss 440668) z-stack images were acquired in 1 μm steps throughout the ventral hemisegment containing rescued muscle cells from the lateral body wall to the midline. For each fluorescent protein of interest, the size of the pinhole was set to 1 airy unit and the laser intensity and gain were adjusted to optimize the detection threshold. The same acquisition parameters were used for subsequent scans across experimental conditions.

Imaris 3D image reconstruction: Confocal images were imported into Imaris and the images were resampled to transform the raw pixel data into cubic, isotropic pixels values. The threshold and pixel intensity for each channel was adjusted to optimize visualization of the fluorescence associated with the labeled cellular component of interest. The arborizations of CaP axon terminal branches were reconstructed using the filament-tracing tool (Wen et al. 2013). Individual 1 μm cylindrical branches were created from a single origin placed on the primary CaP axon branch near the axon's spinal cord exit point. Therefore each axon terminal branch was associated with an exclusive branch terminal point. Muscle cells expressing mCherry were reconstructed using the surfaces tool. Fluorescent puncta associated with αBTX labeled AChRs, FasII labeled AChE and FM1-43 filled presynaptic vesicles were reconstructed using the spots tool.

Quantification of axon terminal branch and synapse number: The number of axon terminal branches throughout the CaP axonal arbor was quantified based on the total number of axon branch terminal points from the 3D reconstructions. The number of synapses on individually identified muscle cells was quantified by counting the number of reconstructed spots associated with fluorescent αBTX puncta that were within 1 μm distance from the muscle's surface. Data are expressed as mean values ± standard deviation (SD).

Results:

α-actin-AChR-δ-P2A-mCherry plasmid suitable for use in partial rescue experiments: The original AChR-δ plasmid that was previously used to successfully rescue AChR expression in *sofa potato* mutants also had cDNA sequences that encoded the cytomegalovirus (CMV) promoter, which drove non-cell-type-specific expression of EGFP (Ono et al. 2004). My experiments required the ability to identify rescued muscles based on the cytoplasmic fluorescence of EGFP in rescued muscle cells and also required that no non-rescued muscle cells express EGFP. I tested this construct by injecting *sofa potato* mutants with α-actin-AChR-δ-CMV-EGFP plasmid and recorded synaptic currents from both fluorescent and nonfluorescent muscle cells at 3, 4 and 5 dpf. I was able to record evoked and miniature EPCs from both EGFP-positive and EGFP-negative muscle cells (data not shown). Thus I could not use this construct for my partial rescue experiments. I turned to creating a different plasmid that would result in muscle fluorescence exclusively in rescued muscles. The new α-actin-AChR-δ-P2A-mCherry plasmid was tested in the same way and proved to work as desired; I was unable to record miniature and evoked EPCs in muscle cells that did not express mCherry fluorescent protein (data not shown). I also qualitatively compared the strength of mCherry muscle fluorescence to the amplitudes of evoked EPCs in rescued muscle cells and observed no relationship between the brightness of the fluorescence and the size of the recorded EPCs (data not shown). Thus, as proof of concept, I found the specificity of mCherry fluorescence in rescued muscles useful for identifying the location of rescued muscle cells for imaging.

Effects of nonuniform AChR expression on CaP axon terminal morphology and the number of synapses on individual muscle cells: In wild-type;SAIG fish, extensive CaP axon terminal branching is seen throughout the ventral muscle field by 72 – 96 hpf (Wen et al. 2015). The number of CaP axon terminal branches had never been quantified; therefore I reconstructed the axon terminal arborization of CaP motor neurons from confocal images acquired at both 3 and 5 dpf using wild-type;SAIG fish and quantified the number of axon terminal branches. To test for changes in CaP axon terminal branch morphology in response to both the absence of AChRs and nonuniform AChR expression throughout the target muscle field, I reconstructed the CaP axon terminal arborizations from non-rescued *sofa potato*;SAIG and partially rescued *sofa potato*;SAIG mutants, respectively, at both 3 and 5 dpf. To probe for evidence of intra-neuronal competition, I first compared the overall structural characteristics of the CaP axon terminal arborizations across the three conditions. There appeared to be no qualitative differences in either overall structure of the axon terminal arbors or axon terminal branch patterning across conditions (Fig. 4A & 4B). Quantitatively, there were no statistically significant differences in the number of axon branches throughout the CaP axon terminal arborizations between both 3 and 5 dpf wild-type;SAIG (WT3 = 48 ± 9, n = 10; WT5 = 63 ± 14, n = 6), non-rescued *sofa potato*;SAIG (*SOP*3 = 43 ± 9, n = 13; *SOP*5 = 53 ± 7, n = 7), and partially rescued *sofa potato*;SAIG fish (*SOP*+δ3 = 48 ± 9, n = 3; *SOP*+δ5 = 47 ± 11, n = 17). Thus data were pooled within each condition to compare across conditions (Fig. 4C; one-way ANOVA, $p = 0.554$). Additionally, there were neither qualitative nor statistically significant quantitative differences between the number of αBTX-568 puncta on individual muscle cells in wild-type fish (29 ± 11, n = 6)

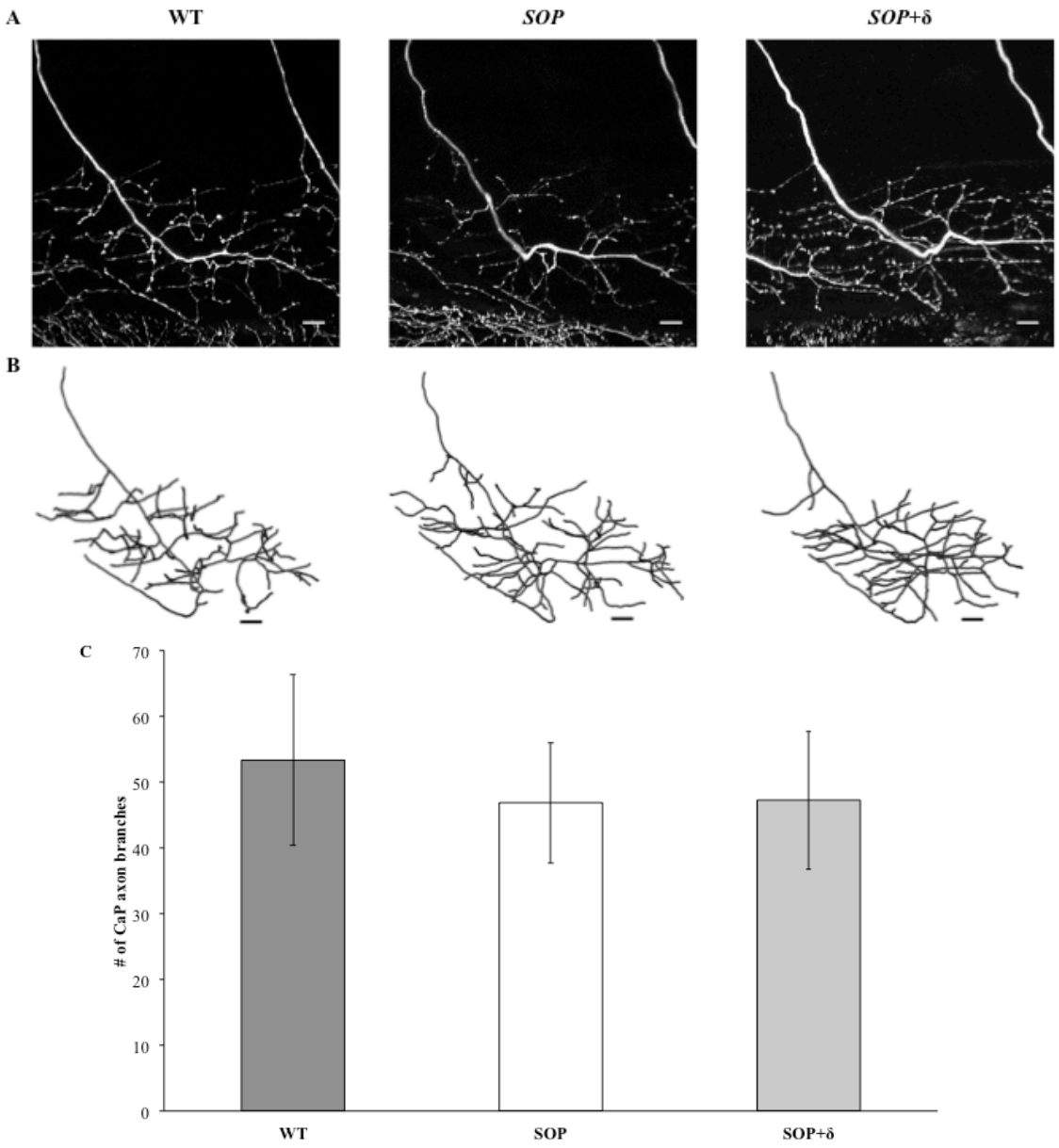

Figure 4. (**A**) Maximum intensity projections of CaP axon terminal branch fluorescence from 1 μm sections acquired throughout the target muscle field. Wild-type (WT), non-rescued *sofa potato* (*SOP*), and partially rescued *sofa potato* (*SOP*+δ). (**B**) Flattened 3D reconstructions of CaP axon terminal branches from stack of fluorescent images (scale bar 10 μm). (**C**) Quantification of the mean number of CaP axon terminal branches across fish conditions (mean ± SD).

and rescued muscle cells in partially rescued *sofa potato* fish (25 ± 10, n = 5) (Fig. 5A – C, t-test, p = 0.526). Accordingly, it appears as though nonuniform AChR expression does not influence CaP axon terminal branch morphology or the number of synapses on individual muscle cells.

Effects of nonuniform AChR expression on the distribution of AChE throughout the CaP target muscle field and on presynaptic vesicle recycling: As there were no differences in the CaP axon terminal branch morphology and number of αBTX puncta on ACh-responsive muscle cells between wild-type and partially rescued *sofa potato* fish, I anticipated the FasII labeling of AChE to be similar between wild-type, non-rescued *sofa potato* and partially rescued *sofa potato* fish. Based on reconstructions of FasII-647 puncta on muscle cells throughout the CaP target muscle field, there appeared to be no qualitative differences from wild-type in the expression patterns of AChE across experimental conditions (Fig. 6A & 6B). Although the data up to this point suggested that nonuniform AChR expression does not influence CaP axon terminal branch morphology, the number of synapses on ACh responsive muscle cells, or the distribution of AChE expression throughout the CaP target muscle field, there was still the possibility that nonuniform AChR expression might have functional consequences in terms of synaptic transmission.

As an optical assay of functional differences in synaptic vesicle recycling, I loaded presynaptic vesicles within the axon terminal boutons of motor neurons with FM1-43. If nonuniform AChR expression influenced presynaptic vesicle recycling, I hypothesized that there would be a compensatory increase in vesicle recycling, thus I

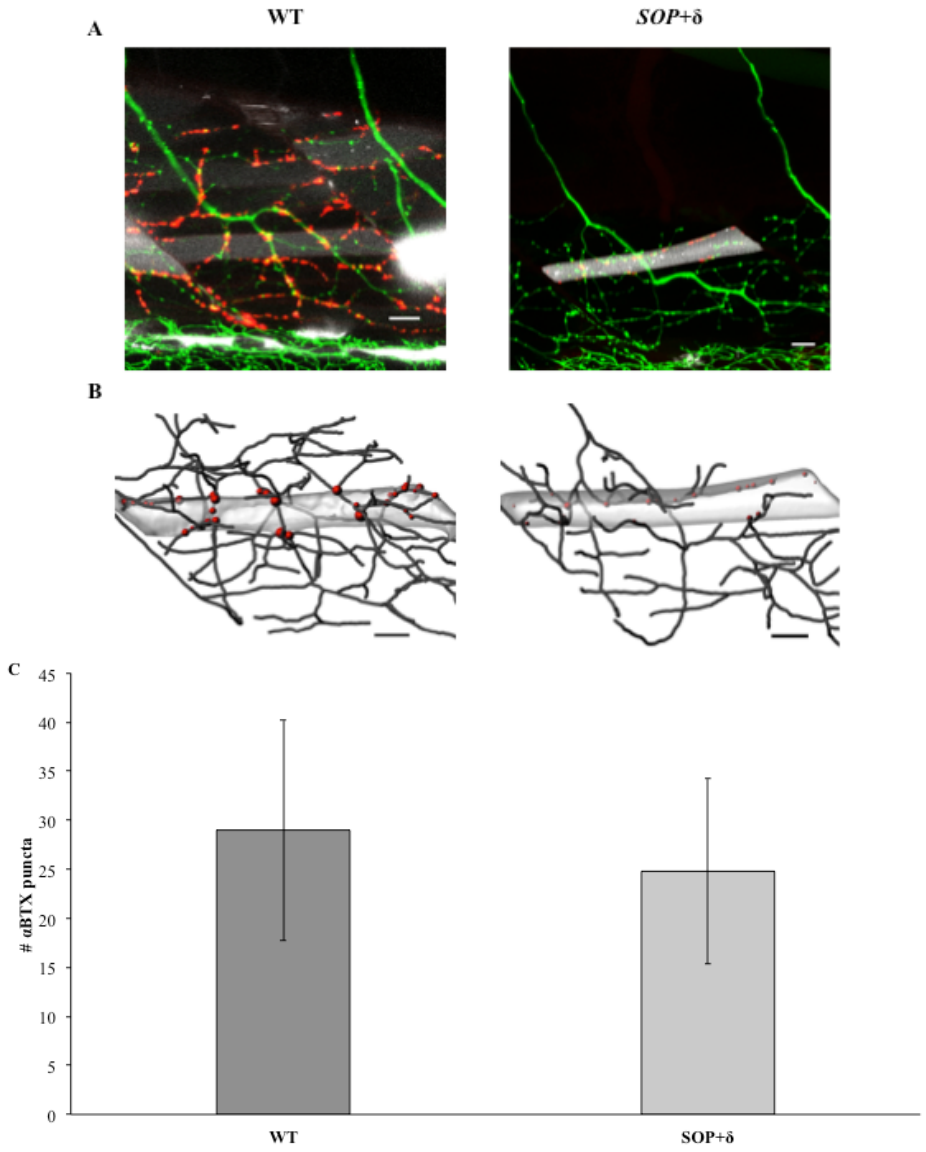

Figure 5. (**A**) Maximum intensity projections of CaP axon terminal branch (green), αBTX-647 labeled AChR (red) and muscle mCherry (white) fluorescence from 1 μm sections acquired throughout the target muscle field. Wild-type (WT), non-rescued *sofa potato* (*SOP*), and partially rescued *sofa potato* (*SOP*+δ). (**B**) Flattened 3D reconstructions of individual muscle cells from stack of fluorescent images (CaP axon terminal branches – black, AChRs – red, and muscle cells – gray) (scale bar 10 μm). (**C**) Quantification of the mean number of αBTX-647 puncta on individually identified muscle cells in wild-type and rescued muscle cells in partially rescued *sofa potato* fish (mean ± SD).

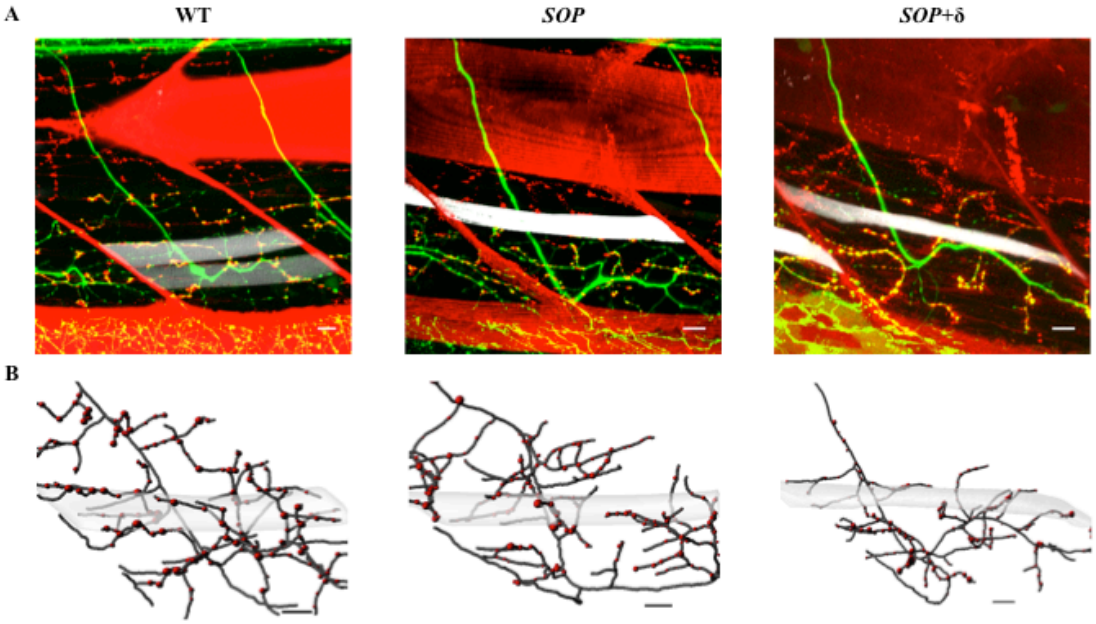

Figure 6. (**A**) Maximum intensity projections of CaP axon terminal branch (green), FasII-647 labeled AChE (red) and muscle mCherry (white) fluorescence from 1 μm sections acquired throughout the target muscle field. Wild-type (WT), non-rescued *sofa potato* (*SOP*), and partially rescued *sofa potato* (*SOP*+δ). (**B**) Flattened 3D reconstructions of individual muscle cells from stack of fluorescent images (CaP axon terminal branches – black, AChE – red, and muscle cells – gray) (scale bar 10 μm).

anticipated there to be greater FM1-43 fluorescence associated with synapses on rescued muscle cells as compared to non-rescued muscle cells in partially rescued *sofa potato* fish. Reconstructions of FM1-43 puncta throughout the ventral muscle field in partially rescued *sofa potato* fish appeared qualitatively similar to wild-type and there did not seem to be any differences in the size or intensity of FM1-43 puncta associated with rescued muscle cells when compared to regions of non-rescued muscle cells (Fig. 7A & 7B).

Conclusions: Based on both quantitative analysis and qualitative assessment, I found that neither the nonuniform expression of AChR protein in muscle cells nor AChR activity at motor endplates to mediate CaP axon terminal branch number and the branching pattern of axons throughout the target ventral muscle field. These findings are contradictory to the earlier reported observations of decreases or increases in synaptic competition under conditions of either diminished or enhanced AChR activity, respectively (Thompson et al. 1979, Thompson 1983). They also differ from findings that motor neurons retracted only from endplate regions where AChR activity was blocked (Balice-Gordon and Lichtman 1994).

On the other hand, my study supports other findings of motor axon outgrowth and branch patterning in zebrafish. Based on the qualitative assessment of the expression patterns of fluorescently labeled motor axons (Westerfield et al. 1990, Ono et al. 2001) or presynaptic terminals (Li et al. 2003) in *sofa potato* mutants, there appeared to be no obvious differences from wild-type controls. In a different study, when either AChR activity was uniformly blocked with αBTX in wild-type fish or AChR activity and AChR

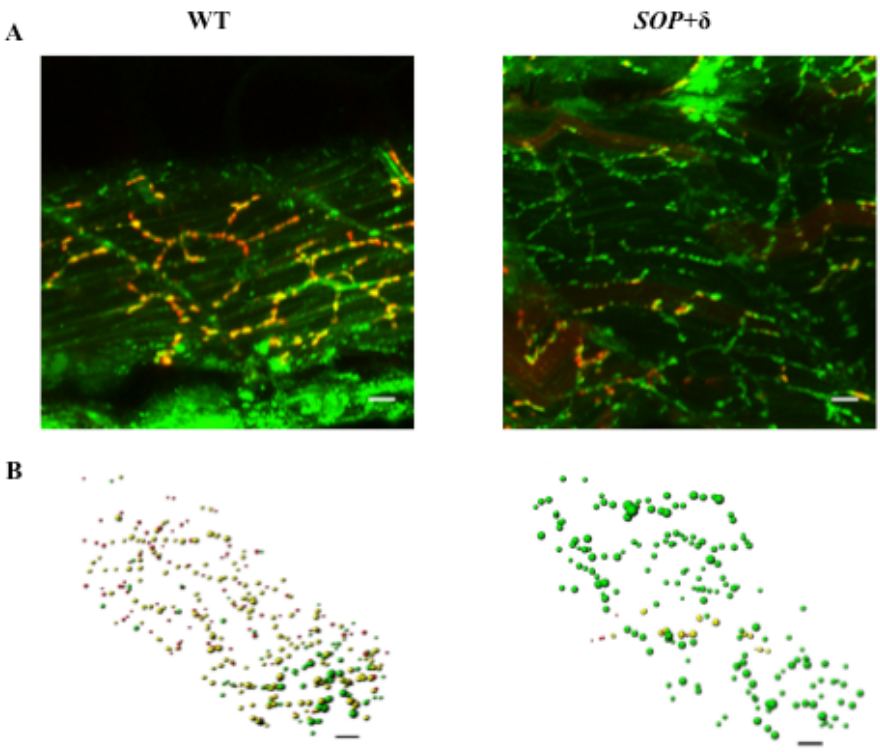

Figure 7. (**A**) Maximum intensity projections of motor neuron presynaptic vesicles loaded with FM1-43 (green) and αBTX-647 labeled AChR (red) fluorescence from 1 µm sections acquired throughout the target muscle field. Wild-type (WT) and partially rescued *sofa potato* (*SOP*+δ). (**B**) Flattened 3D reconstructions of individual ventral muscle field from stack of fluorescent images (FM1-43 – green, AChRs – red, and colocalized FM1-43 and AChRs – yellow) (scale bar 10 µm).

protein were uniformly absent in *sofa potato* mutants, there was no difference in the outgrowth of motor axons (Panzer et al. 2006). This suggests that, in zebrafish, primary motor axons project throughout their target muscle fields responding to other cell-cell signaling cues at the end plate that are independent of AChR-activity.

Additionally, based on αBTX expression, my findings show that the number of synapses on ACh-responsive muscle cells is independent of both AChR protein expression and AChR activity. One thing that remains unknown is whether there are changes in synaptic transmission in response to nonuniform AChR expression. Our lab has recently completed a study of synaptic transmission at the zebrafish neuromuscular junction using a different mutant line that has diffuse AChR expression due to a mutation in rapsyn, which controls AChR clustering (Wen et al. 2016). There were two main findings attributed to the reduced AChR density opposite presynaptic terminals. First, was an increase in transmitter release that resulted from an increase in quantal content, reflecting a greater number of vesicles released per action potential. The increase in quantal content was further shown to result from an increased number of release sites. To our surprise, the second effect of reduced AChR density ran counter to the compensatory increase in the number of release sites. Measurements of exocytosis using an optical indicator showed that release was compromised at individual release sites during repetitive stimulation. These studies highlight that differential levels of AChRs can mediate changes in presynaptic transmission. Future studies could test for changes in quantal content and exocytosis from the CaP motor neuron onto rescued muscles in partially rescued *sofa potato* mutants.

Although my findings did not support my hypotheses, the methods I used throughout my study led to the development of useful tools for the lab. In addition to mastering the paired motor-neuron target muscle patch clamp recording technique, I employed several molecular cloning techniques to develop a plasmid that can be used to optically identify individual muscle cells that express AChRs in *sofa potato* mutant zebrafish. The specificity of this plasmid is the exact tool required for testing if nonuniform AChR expression throughout the CaP target muscle field results in changes in synaptic transmission.

I also generated a transgenic *sofa potato* synapto-pHluorin fish line (*sofa potato*;zpH), which expresses a pH-sensitive fluorescent protein that provides a direct indication of vesicle exocytosis exclusively in CaP motor neurons (Wen et al. 2013, Miesenbock et al. 1998). Using the AChR-δ plasmid I designed to partially rescue *sofa potato*;zpH mutants would allow for testing if nonuniform AChR expression results in changes in vesicle exocytosis.

I have also become competent in the acquisition of multi-color confocal z-stack images and 3D image reconstruction. This has allowed me to gather data sets for a grant application and another project in the lab studying the morphological characteristics of secondary motor neurons and the relationship between primary-secondary and secondary-secondary motor neurons that share same target muscle field. Moreover, my contribution to this study will hopefully corroborate the findings from future electrophysiological experiments, to see if the size-ordered recruitment of motor neurons of Henneman's size principle also applies in zebrafish (Henneman et al. 1965).

Throughout my graduate training, my intellectual awareness has matured, providing me with the faculties necessary for objectively resolving complex problems and achieving my personal and professional goals. I now have a greater understanding of the importance of networking with my colleagues and asking for assistance from those more experienced to increase the efficiency of my work. I also have greater confidence in my ability to critically evaluate information sources when researching questions and both my patience and perseverance while working through challenging tasks have enhanced my ability to remain focused and not give up on a project prematurely.

Finally, attempting to follow in the footsteps of the experimental embryologist Hans Spemann, who's use of his daughter's fine baby hair to study salamander embryogenesis in the early 1900's led to his winning a Nobel prize (Fässler 1996), I too have found a use for hair in science. After testing different hair types, I found the nose-hair to be the perfect instrument for the removal of dorsal muscle fibers in juvenile zebrafish, in order to access the spinal cord for electrophysiological recordings of spinal motor neurons. The carefully selected nose-hair has an ideal hooked-curvature shape and amount of elasticity, which allows for precision muscle removal with minimal risk of damaging the dura of the spinal cord and surrounding muscle tissue. Compared to the lab-standard electrolytically sharpened and bent tungsten rod, I feel the nose-hair is the superior muscle dissection instrument. Well aware that my application of nose-hairs in science will not lead to my achieving Nobel laureate status, I hope that one day someone else in the lab will take my suggestion of using nose-hairs for this purpose.

References

Axelsson, J. and S. Thesleff (1959). "A study of supersensitivity in denervated mammalian skeletal muscle." J Physiol **147**(1): 178-193.

Balice-Gordon, R. J. and J. W. Lichtman (1994). "Long-term synapse loss induced by focal blockade of postsynaptic receptors." Nature **372**(6506): 519-524.

Beattie, C. E. (2000). "Control of motor axon guidance in the zebrafish embryo." Brain Res Bull **53**(5): 489-500.

Berg, D. K. and Z. W. Hall (1975). "Increased extrajunctional acetylcholine sensitivity produced by chronic acetylcholine sensitivity produced by chronic post-synaptic neuromuscular blockade." J Physiol **244**(3): 659-676.

Brown, G. L. (1937). "The actions of acetylcholine on denervated mammalian and frog's muscle." J Physiol **89**(4): 438-461.

Brown, M. C., J. K. Jansen and D. Van Essen (1976). "Polyneuronal innervation of skeletal muscle in new-born rats and its elimination during maturation." J Physiol **261**(2): 387-422.

Burden, S. (1977). "Acetylcholine receptors at the neuromuscular junction: developmental change in receptor turnover." Dev Biol **61**(1): 79-85.

Colman, H. and J. W. Lichtman (1993). "Interactions between nerve and muscle: synapse elimination at the developing neuromuscular junction." Dev Biol **156**(1): 1-10.

Davis, G. W. and M. Muller (2015). "Homeostatic control of presynaptic neurotransmitter release." Annu Rev Physiol **77**: 251-270.

del Castillo, J. and G. Escalona de Motta (1978). "A new method for excitation-contraction uncoupling in frog skeletal muscle." J Cell Biol **78**(3): 782-784.

Epley, K. E., J. M. Urban, T. Ikenaga and F. Ono (2008). "A modified acetylcholine receptor delta-subunit enables a null mutant to survive beyond sexual maturation." J Neurosci **28**(49): 13223-13231.

Fässler, P. E. (1996). "Hans Spemann (1869-1941) and the Freiburg School of Embryology." Int J Dev Biol **40**(1): 49-57.

Henneman, E., G. Somjen and D. O. Carpenter (1965). "Functional Significance of Cell Size in Spinal Motoneurons." J Neurophysiol **28**: 560-580.

Higashijima, S., H. Okamoto, N. Ueno, Y. Hotta and G. Eguchi (1997). "High-frequency generation of transgenic zebrafish which reliably express GFP in whole muscles or the whole body by using promoters of zebrafish origin." Dev Biol **192**(2): 289-299.

Ibanez-Tallon, I., H. Wen, J. M. Miwa, J. Xing, A. B. Tekinay, F. Ono, P. Brehm and N. Heintz (2004). "Tethering naturally occurring peptide toxins for cell-autonomous modulation of ion channels and receptors in vivo." Neuron **43**(3): 305-311.

Kano, M. and K. Hashimoto (2009). "Synapse elimination in the central nervous system." Curr Opin Neurobiol **19**(2): 154-161.

Kim, J. H., S. R. Lee, L. H. Li, H. J. Park, J. H. Park, K. Y. Lee, M. K. Kim, B. A. Shin and S. Y. Choi (2011). "High cleavage efficiency of a 2A peptide derived from porcine teschovirus-1 in human cell lines, zebrafish and mice." PLoS One **6**(4): e18556.

Li, W., F. Ono and P. Brehm (2003). "Optical measurements of presynaptic release in mutant zebrafish lacking postsynaptic receptors." J Neurosci **23**(33): 10467-10474.

McMahan, U. J., J. R. Sanes and L. M. Marshall (1978). "Cholinesterase is associated with the basal lamina at the neuromuscular junction." Nature **271**(5641): 172-174.

Miesenbock, G., D. A. De Angelis and J. E. Rothman (1998). "Visualizing secretion and synaptic transmission with pH-sensitive green fluorescent proteins." Nature **394**(6689): 192-195.

Mishina, M., T. Takai, K. Imoto, M. Noda, T. Takahashi, S. Numa, C. Methfessel and B. Sakmann (1986). "Molecular distinction between fetal and adult forms of muscle acetylcholine receptor." Nature **321**(6068): 406-411.

Mongeon, R., M. Walogorsky, J. Urban, G. Mandel, F. Ono and P. Brehm (2011). "An acetylcholine receptor lacking both gamma and epsilon subunits mediates transmission in zebrafish slow muscle synapses." J Gen Physiol **138**(3): 353-366.

Ono, F., S. Higashijima, A. Shcherbatko, J. R. Fetcho and P. Brehm (2001). "Paralytic zebrafish lacking acetylcholine receptors fail to localize rapsyn clusters to the synapse." J Neurosci **21**(15): 5439-5448.

Ono, F., G. Mandel and P. Brehm (2004). "Acetylcholine receptors direct rapsyn clusters to the neuromuscular synapse in zebrafish." J Neurosci **24**(24): 5475-5481.

Pestronk, A., D. B. Drachman and J. W. Griffin (1976). "Effect of muscle disuse on acetylcholine receptors." Nature **260**(5549): 352-353.

Plomp, J. J., G. T. van Kempen and P. C. Molenaar (1992). "Adaptation of quantal content to decreased postsynaptic sensitivity at single endplates in alpha-bungarotoxin-treated rats." J Physiol **458**: 487-499.

Redfern, P. A. (1970). "Neuromuscular transmission in new-born rats." J Physiol **209**(3): 701-709.

Robbins, N. and G. D. Fischbach (1971). "Effect of chronic disuse of rat soleus neuromuscular junctions on presynaptic function." J Neurophysiol **34**(4): 570-578.

Slater, C. R. (2015). "The functional organization of motor nerve terminals." Prog Neurobiol **134**: 55-103.

Thompson, W. (1983). "Synapse elimination in neonatal rat muscle is sensitive to pattern of muscle use." Nature **302**(5909): 614-616.

Thompson, W., D. P. Kuffler and J. K. Jansen (1979). "The effect of prolonged, reversible block of nerve impulses on the elimination of polyneuronal innervation of new-born rat skeletal muscle fibers." Neuroscience **4**(2): 271-281.

Turrigiano, G. (2012). "Homeostatic synaptic plasticity: local and global mechanisms for stabilizing neuronal function." Cold Spring Harb Perspect Biol **4**(1): a005736.

Turrigiano, G. G. and S. B. Nelson (2004). "Homeostatic plasticity in the developing nervous system." Nat Rev Neurosci **5**(2): 97-107.

Walogorsky, M., R. Mongeon, H. Wen, G. Mandel and P. Brehm (2012). "Acetylcholine receptor gating in a zebrafish model for slow-channel syndrome." J Neurosci **32**(23): 7941-7948.

Wen, H. and P. Brehm (2005). "Paired motor neuron-muscle recordings in zebrafish test the receptor blockade model for shaping synaptic current." J Neurosci **25**(35): 8104-8111.

Wen, H. and P. Brehm (2010). "Paired patch clamp recordings from motor-neuron and target skeletal muscle in zebrafish." J Vis Exp(45).

Wen, H., J. M. Hubbard, B. Rakela, M. W. Linhoff, G. Mandel and P. Brehm (2013). "Synchronous and asynchronous modes of synaptic transmission utilize different calcium sources." Elife **2**: e01206.

Wen, H., J. M. Hubbard, W. C. Wang and P. Brehm (2016). "Fatigue in Rapsyn-Deficient Zebrafish Reflects Defective Transmitter Release." J Neurosci **36**(42): 10870-10882.

Wen, H., M. J. McGinley, G. Mandel and P. Brehm (2015). "Nonequivalent release sites govern synaptic depression." Proc Natl Acad Sci U S A **113**(3): E378-386.

Westerfield, M., D. W. Liu, C. B. Kimmel and C. Walker (1990). "Pathfinding and synapse formation in a zebrafish mutant lacking functional acetylcholine receptors." Neuron **4**(6): 867-874.

Westerfield, M., J. V. McMurray and J. S. Eisen (1986). "Identified motoneurons and their innervation of axial muscles in the zebrafish." J Neurosci **6**(8): 2267-2277.

Witzemann, V., F. Chevessier, P. G. Pacifici and P. Yampolsky (2013). "The neuromuscular junction: selective remodeling of synaptic regulators at the nerve/muscle interface." Mech Dev **130**(6-8): 402-411.

Wyatt, R. M. and R. J. Balice-Gordon (2003). "Activity-dependent elimination of neuromuscular synapses." J Neurocytol **32**(5-8): 777-794.